



ARTICLE

Microstructural Dependence of Friction and Wear Behavior in Biological Shells

Xin Wang^{1,3}, Ying Yan^{1,3}, Hongmei Ji^{1,3,*} and Xiaowu Li^{1,2,*}

¹Department of Materials Physics and Chemistry, School of Material Science and Engineering, Northeastern University, Shenyang, 110819, China

²State Key Laboratory of Rolling and Automation, Northeastern University, Shenyang, 110819, China

³Key Laboratory for Anisotropy and Texture of Materials, Ministry of Education, Northeastern University, Shenyang, 110819, China

*Corresponding Authors: Hongmei Ji. Email: jihongmei@mail.neu.edu.cn; Xiaowu Li. Email: xwli@mail.neu.edu.cn

Received: 12 October 2022 Accepted: 13 December 2022 Published: 26 June 2023

ABSTRACT

As an essential renewable mineral resource, mollusk shells can be used as handicrafts, building materials, adsorbents, etc. However, there are few reports on the wear resistance of their structures. The Vicker's hardness and friction, and wear resistance of different microstructures in mollusk shells were comparatively studied in the present work. The hardness of prismatic structures is lower than that of cross-lamellar and nacreous structures. However, the experimental results of sliding tests indicate that the prismatic structure exhibits the best anti-wear ability compared with foliated, crossed-lamellar, and nacreous structures. The anti-wear and hardness do not present a positive correlation, as the wear resistance properties of different microstructures in mollusk shells are governed jointly by organic matrix, structural arrangement, and basic building block actions. The present research findings are expected to provide fundamental insight into the design of renewable bionic materials with high wear resistance.

KEYWORDS

Mollusk shells; microstructure; hardness; friction; wear

1 Introduction

Since the phenomenon of friction and wear spreads across all kinds of machinery and causes considerable losses to the national economy, many works have focused on the investigations of the friction and wear properties of materials [1]. Compared with artificial materials, some natural biological materials usually show good wear resistance in addition to high strength and toughness [2,3].

It is well known that natural biomaterials not only provide guidelines for human inventions at the macro level but also offer inspiration for the design of high-performance materials at the micro level due to their specific microstructural construction [4–6]. As an important renewable mineral resource, the conversion and utilization of mollusk shells have attracted considerable attention [7]. The full development and utilization of abundant mollusk shell resources not only increase the added value and realize the recycling and reduction of wastes but also promote the healthy development of shellfish farming and increase the carbon sink capacity of marine resources. It has been recognized that there are seven kinds of microstructures in shells (including crossed-lamellar, complex crossed-lamellar, prismatic, sheet nacre,



columnar nacre, foliated and homogeneous structures), and there are significant differences in the structural arrangement of different microstructures [8]. So far, most studies focus on the friction and wear performance of shells with different outer surface morphologies under different external conditions or that of a specific microstructure or a particular shell under various external conditions [9–11]. For instance, Tong et al. [9] reported that the direction of the corrugations on the outer surface of shells had a more significant impact on the friction and wear resistance under different external environments. Stempflié et al. [10] studied the friction and wear properties of nacre in dry conditions and liquid media, respectively, and found that various external environments had different effects on the wear behavior of materials. Lv et al. [11] showed that the friction and wear properties of the cuticle, nacreous and prismatic layers within the same mollusk shell depended significantly on their different microstructures under dry conditions and liquid media. However, systematic study concerning the comparison of friction and wear resistance of different microstructures in mollusk shells is still lacking.

Therefore, several common types of microstructures in natural shells have been selected as the target materials, and their hardness and anti-wear behaviors have been investigated to find the microstructure with the best resistance to friction and wear, and thus provide a novel guideline for the biomimetic fabrication of renewable friction-reduction and anti-wear materials.

2 Materials and Methods

The hard shells of five mollusk species are selected as the target materials in the present work, including *Cassis cornuta* from the South China Sea (Fig. 1a), *Hyriopsis cumingii* from Henan, China (Fig. 1b), *Pinctada margaritifera* from Tahiti in Polynesia (Fig. 1c), *Red Abalone* from California, USA (Fig. 1d), and *Placuna placenta* from the East China Sea (Fig. 1e). The entire *P. placenta* shell is highly transparent in contrast to the other shells [12,13]. All the shells were purchased from a material supplier. The microstructures along different directions of these shells were observed by scanning electron microscopy (SEM). The inorganic crystalline phase of these shells was analyzed using an X-ray diffraction machine with CuK α radiation at 45 kV and 40 mA.

The microhardness of five types of microstructures in mollusk shells was evaluated by using a Vickers hardness tester (TMV-1) at a load of 200 g and a dwelling time of 15 s. The tribometer friction and wear testing machine produced by NANOVEA company was used to study the friction and wear properties of five types of microstructures. Three groups of parallel samples were prepared. Square samples of 10 mm \times 10 mm are cut from the mollusk shells, and the large face of all the samples is parallel to the outer surfaces of the shells, as illustrated in Figs. 1f–1j. The samples are smoothed by rough and fine grinding, and then mechanically polished with 0.5 μ m diamond abrasion paste. The friction and wear tests were carried out on these samples in a dry condition for 15 min under a speed of 160 rpm and a load of 8 N. For *P. placenta* sample. The experimental time is set as 5 min since its shell is obviously thinner than the other shells. The thickness of the *P. placenta* sample in Fig. 1j is \sim 1.0 mm, and the other four samples are \sim 2.5 mm. The friction pair is a SiC sphere with a diameter of 6 mm. The relative sliding length of the friction pair is 6 mm. Fig. 1k shows the schematic diagram of the friction-wear tester. Wear tracks and morphologies of the surface were analyzed using a laser scanning confocal microscope (LSCM) and SEM. The mass of the samples before and after wear was measured with an MT-ME204 electronic scale with an accuracy of 0.01 mg. The weight loss rate was calculated as follows:

$$\eta = \frac{W_0 - W_b}{W_0} \quad (1)$$

where W_0 and W_b represent the sample mass before and after wear tests, respectively.

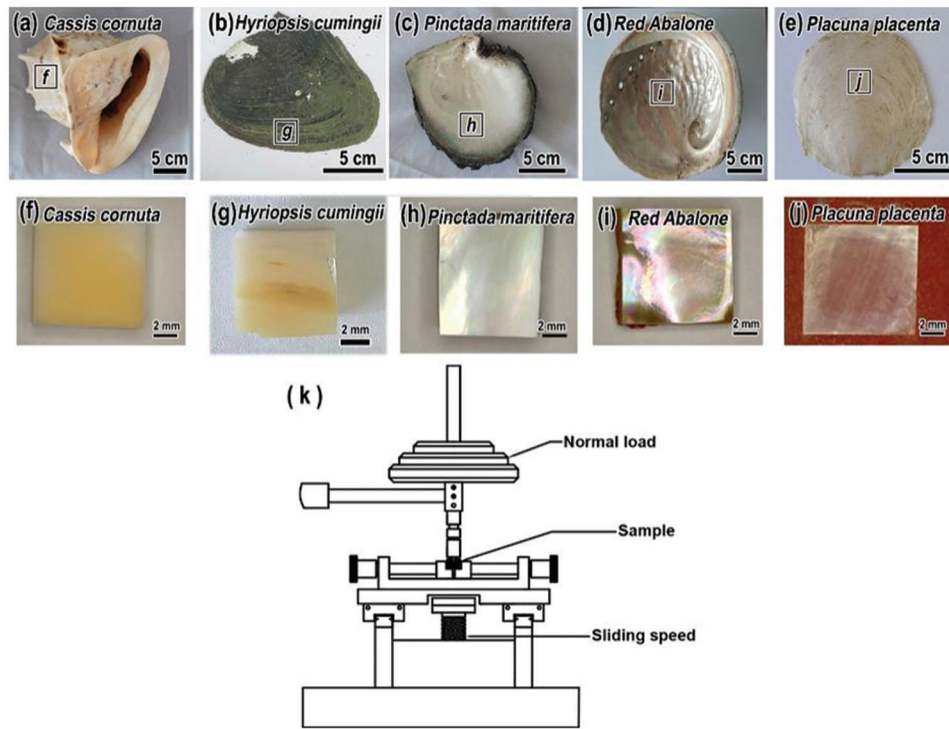


Figure 1: Morphologies and samples for friction and wear tests of *C. cornuta* (a, f), *H. cumingii* (b, g), *P. margaritifera* (c, h), *R. Abalone* (d, i), and *P. placenta* (e, j) shells, and (k) schematic diagram of the friction-wear tester

3 Results and Discussion

3.1 Microstructure

Figs. 2a and 2f give the SEM morphologies of the *C. cornuta* shell, and it presents a crossed-lamellar structure, in which the fibers in the adjacent lamellae are aligned in different directions (Fig. 2a). It is observed that the fibers in the adjacent lamellae are perpendicular to each other, showing a kind of natural composite with fiber-reinforced and cross-ply laminates (Fig. 2f). Figs. 2b and 2g give the SEM image of the exterior layer in *H. cumingii* shell, and it is found that this layer shows a prismatic structure, and the prisms are unusually large with a diameter of 10–60 μm (Fig. 2b) and a length of hundreds of microns (Fig. 2g). Figs. 2c and 2h show the microstructure of the inner layer in *P. margaritifera* shell, which exhibits a sheet nacre structure, and the platelets in this structure present a hexagonal shape (Fig. 2c). The upper platelets span the interfaces of the underlying platelets, presenting a “brick wall” morphology (Fig. 2h). Figs. 2d and 2i are the microstructures of *Red Abalone*, and it is composed of a columnar nacre structure, and the platelets in this structure also have a hexagonal shape (Fig. 2d). The platelets show a roughly uniform size and the centers of the platelets are coincident (Fig. 2i). The shell of *P. placenta* mainly presents a foliated structure, as shown in Figs. 2e and 2j. The folia are usually inclined at an angle lower than 10° to the surface of the shell, presenting a “fish scales” morphology (Fig. 2e). Besides, the thickness of the folia is extremely thin (Fig. 2j). XRD analysis reveals that the crossed-lamellar structure, prismatic, sheet nacre, and columnar nacre are composed of aragonite calcium carbonate, while the foliated structure consists of calcite calcium carbonate, as shown in Fig. 2k. The mineral phase of four types of structures keeps the same, except for the foliated structure as it only has one type of mineral phase. In such a way, the comparison of the influence of different microstructures on friction and wear behavior of shells is exacter. Mollusk shells are mainly composed of mineral phase and

a few percent of organic matrix. The previous investigations have indicated that the organic content is more than 4 wt.% in prismatic structure [14], 3–4 wt.% in nacreous structure [15], 1–2 wt.% in crossed-lamellar structure [16], and less than 1 wt.% in foliated structure [17].

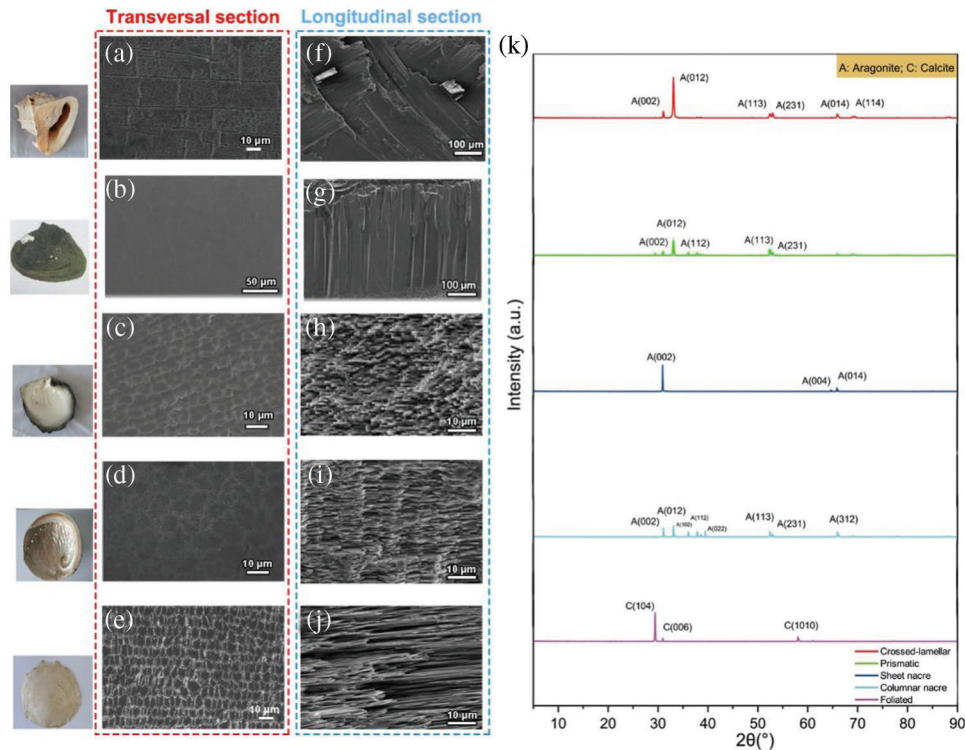


Figure 2: Morphologies on the transversal and longitudinal sections of the crossed-lamellar (a, f), prismatic (b, g), sheet nacre (c, h), columnar nacre (d, i), and foliated (e, j), respectively, and (k) the XRD spectra of five types of microstructures

3.2 Hardness

The Vicker's hardness of five types of microstructures in mollusk shells is shown in Fig. 3. It can be seen that the nacreous structures exhibit the highest hardness, i.e., the hardness of sheet nacre in the *P. margaritifera* shell is ~287 HV, and it is a little higher than that (262 HV) of the columnar nacre in *R. Abalone* shell. The hardness of the crossed-lamellar structure in the *C. cornuta* shell and the prismatic structure in the *H. cumingii* shell is comparable, which presents a value of 246 HV and 252 HV, respectively. The foliated structure shows the lowest hardness (189 HV). It should note that the distribution of the hardness of different shells does not show an obvious relationship with the organic matter content. For example, the crossed-lamellar and foliated structures both present a ~1 wt.% organic matter content, but the crossed-lamellar structure is much harder than the foliated structure. Therefore, the microstructures play important roles in the hardness of shell materials. It can be seen that the platelet arrangement is more complicated in sheet nacre, which results in higher hardness.

3.3 Anti-Wear Ability of Different Microstructures

Fig. 4 gives the coefficient of friction (COF) and mass wear rate of five types of microstructures in mollusk shells, respectively. It can be seen that the friction coefficient of each structure increases, and finally keeps stable with time increasing (Fig. 4a). The COF of samples presents a stage with a slow

growth rate at the very beginning of the tests except for the *P. placenta* sample, and this stage is wide, especially for the crossed-lamellar and prismatic structure. In contrast, the COF increases directly and rapidly in the *P. placenta* sample, indicating that the sample is damaged immediately once the test starts. Some fluctuations can be observed in the experimental curves, which are attributed to the existence of detached particles and oxides in the contact [18–21]. The friction coefficients of the crossed-lamellar and foliated structures are greater than those of the other structures, as shown in Fig. 4a. For nacreous structures, the friction coefficient of columnar nacre is greater than that of sheet nacre. Furthermore, the prismatic structure has the lowest COF among the five structures. Although the friction and wear time of the foliated structure is only one-third that of the other four types of structures, its mass wear rate is much higher among the structures. In sharp contrast, the mass wear rate of the prismatic structure is an order of magnitude lower than that of the other four types of structures (Fig. 4b). In other words, under the same external conditions, there are many differences in the resistance to friction and wear deformation for different structures.

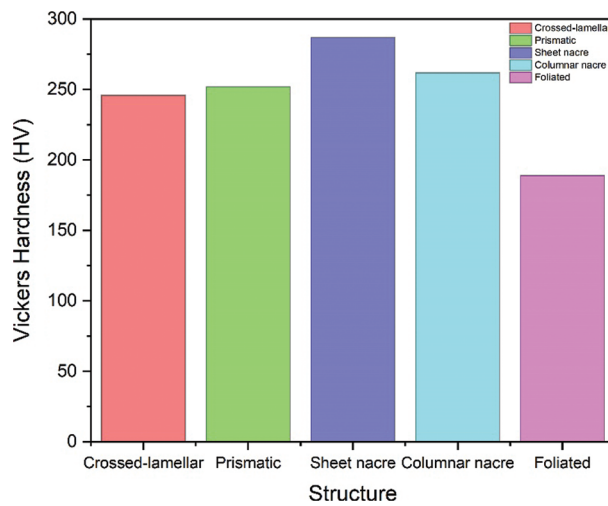


Figure 3: Hardness of crossed-lamellar, prismatic, sheet nacre, columnar nacre and foliated structure in mollusk shells

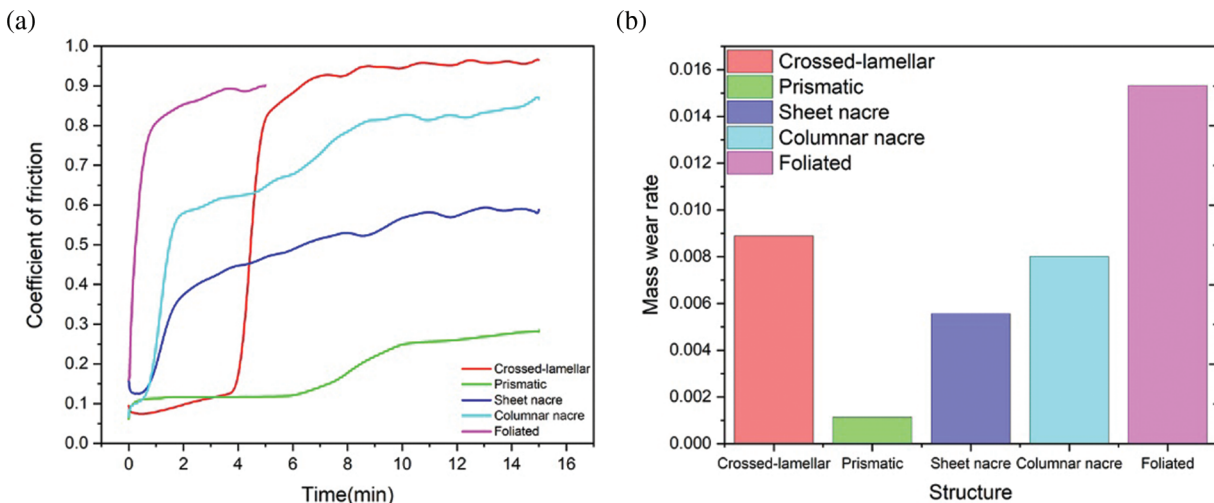


Figure 4: Coefficient of friction (a) and mass wear rate (b) of five types of microstructures

The topographies and the cross-section profiles of the wear tracks obtained with the confocal profilometer are shown in Fig. 5. Figs. 5a, 5e, and 5f clearly show that the foliated and crossed-lamellar structures present larger tracks. The foliated structure exhibits the deepest track ($\sim 300 \mu\text{m}$), although the friction and wear time is one-third that of the other four types of structures (Fig. 4a). Such phenomena indicate that the foliated structure is the worst to resist friction and wear. The wear track morphologies of sheet nacre and columnar nacre are similar, but the depth of the track of columnar nacre is larger than that of sheet nacre (Figs. 5c, 5d, and 5f). In contrast, the wear track depth of the prismatic structure is evidently lower than those of the other structures, and no serious wear is observed on its surface (Figs. 5b and 5f). That is to say, the friction and wear resistance of the foliated structure is the worst, but the prismatic structure is the best among the five types of structures.

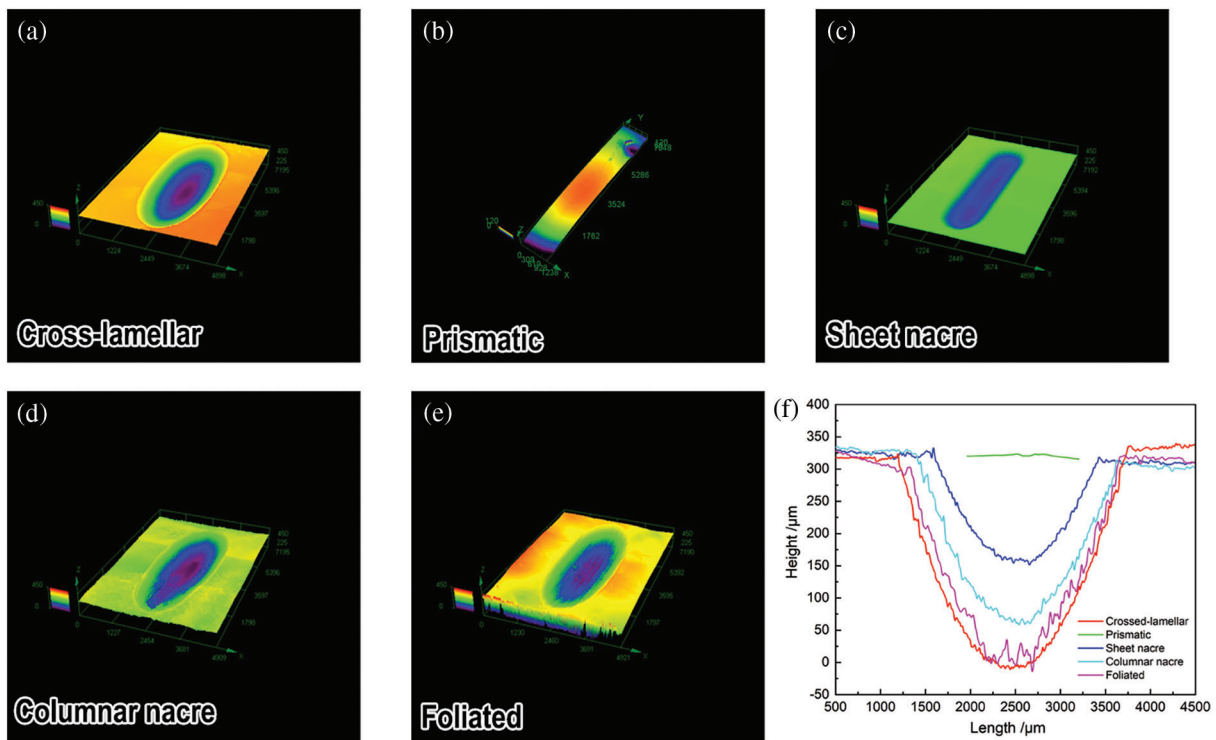


Figure 5: LSCM of the wear tracks of crossed-lamellar (a), prismatic (b), sheet nacre (c), columnar nacre (d), and foliated (e) structures in friction and wear tests, and (f) cross-section profiles of the wear tracks obtained in friction and wear tests

Fig. 6 shows SEM characterization of the topographies of the wear tracks of the crossed-lamellar structure and foliated structure. The wear track surfaces in the crossed-lamellar structure represent a typical fatigue fracture wear and plastic deformation wear with plough and some cracks, as shown in Figs. 6a–6c. Also, more fractures can be clearly seen in the edges (Fig. 6c). In comparison to the crossed-lamellar structure, more fracturing and ploughing are observed on the wear track surfaces of the foliated structure (Figs. 6d–6f). Besides, it is noted that fracture failure emerges almost on all of the edges of samples, which may be the main factor causing higher friction coefficient and mass wear rate in foliated structure (Fig. 6f). That is to say, the surface first undergoes evident plastic deformation, and eventually, cracks are formed at the edges of defects and stress concentration sites on the surfaces, further causing a fracture failure. The organic matrix content of these two types of structure is obviously low, and their wear tracks present the biggest depth, which may illustrate that the organic matrix can contribute to the friction and wear resistance of materials.

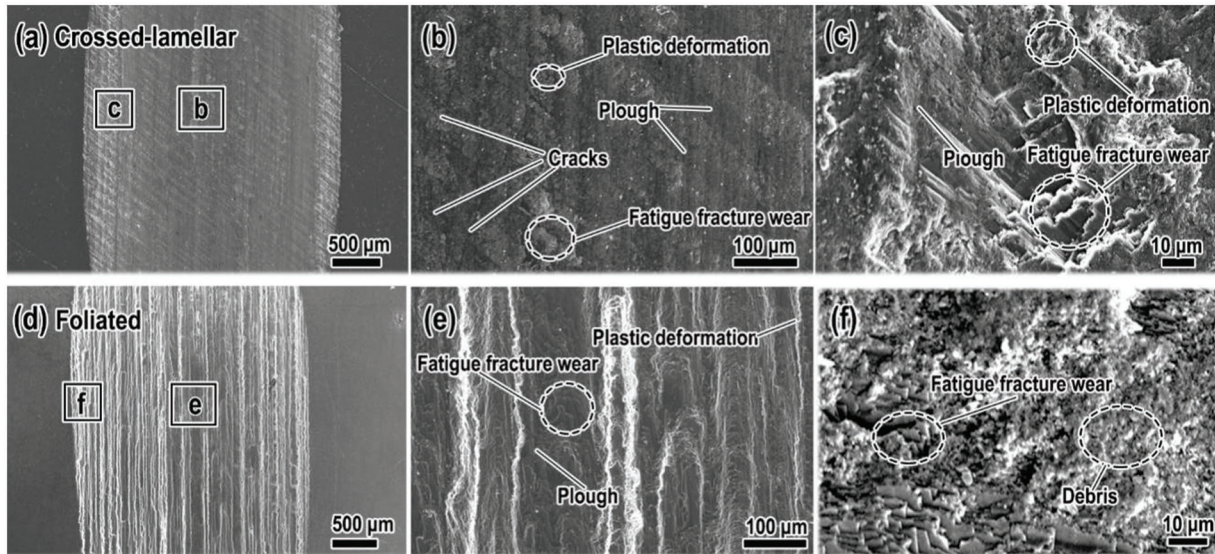


Figure 6: SEM characterization of the topographies of the wear tracks generated in friction and wear tests of crossed-lamellar structure (a–c), and foliated structure (d–f)

Comparing the topographies of the nacreous structures in Fig. 7, it can be observed that the surfaces of the wear track from the sheet nacre structure represent a typical fatigue fracture wear and a plastic deformation wear with many peeling layers and fine debris, as shown in Figs. 7a, 7b, whereas the surfaces of wear track from the columnar nacre exhibit a typical fatigue fracture wear and a plastic deformation wear with larger regularly arranged plough (like-hills) and some debris, as shown in Figs. 7c, 7d. So, the different arrangements of nacreous structures result in different forms of the plough, indicating that the different arrangements of nacreous structures provide different wear mechanisms.

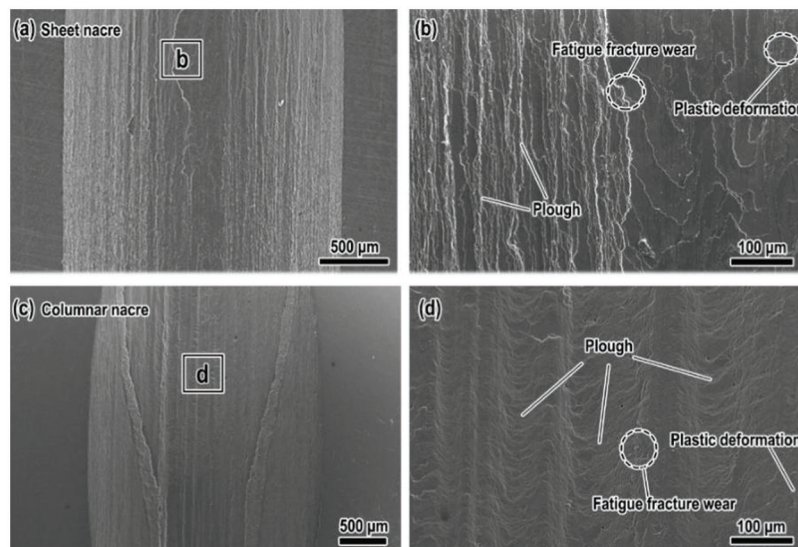


Figure 7: SEM characterization of the topographies of the wear tracks generated friction and wear tests of sheet nacre structure (a, b), and columnar nacre structure (c, d)

Fig. 8 shows the SEM characterizations of the topography of the wear tracks of the prismatic structure generated in friction and wear tests. The micro-cutting wear and plastic deformation wear with a bit of ploughs and micro-pits on the worn surface are observed, indicating that a small amount of damage is introduced. Therefore, the wear is weaker in the prismatic structure. The composition in the interfaces between prisms is evidently fallen away (Fig. 8c). In the prismatic structure, the organic matrix content is higher and they mainly locate on the interfaces among prisms [22,23]. The interprismatic organic membranes may act as a kind of lubricant, thus effectively protecting the prisms from wear and friction damage.

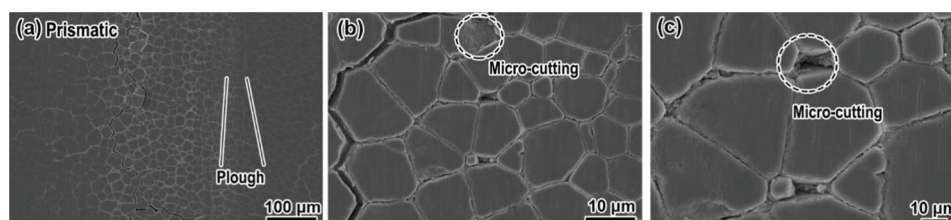


Figure 8: SEM characterization of the topography of the wear tracks generated in friction and wear tests of prismatic structure

It is well known that metallic materials with a higher hardness can exhibit better anti-wear, which originates from the compactness of metallic materials and better bonding strength of grain boundaries [24–26]. However, in the current work, it is revealed that the higher hardness does not exactly correspond to higher wear resistance in mollusk shells, since the wear resistance properties of the different microstructures are the result of interactions of organic matrix, structural arrangement, and basic building block. During wear, the organic matrix will be moved to the friction interface, hence forming an organic film. The organic film will lubricate the friction interface and thus protect the friction surface, which makes the mollusk shells present great friction and wear resistance [25]. The content of organic matrix in prismatic structure is the highest among the five kinds of structures, which has a positive influence on friction and wear resistance. Besides, a relatively high hardness may effectively restrain the crack propagation, thus avoiding fatigue fracture wear [26].

The schematic abrasion mechanism and the abrasive penetration effect are clearly shown in Fig. 9. Since the crossed-lamellar structure is composed of tiny fibers [27,28], it is easily damaged during wear. Furthermore, the lamellae are parallel to each other [29], which leads to the formation of the regular fracture and plough in some areas, and thus makes it to be worn severely (Fig. 9a).

The prismatic structure is the most important feature of the *H. cumingii*'s exterior. The prismatic units consist of large and long calcite that are surrounded by thick organic walls, and they are perpendicular to the shell faces [30,31]. The organic envelope lubricated the friction interface and the large and long prismatic aragonite protects the friction surface, which promotes the formation of only a few ploughs and micro-cutting wear in this layered structure [23]. Therefore, the prismatic structure shows particular resistance to wear (Fig. 9b).

The platelets in columnar nacre are arranged in columns with well-defined cores, and they have a quasi-periodic structure [32,33]. In this way, the interfaces of the edge faces of the platelets are more easily to be cracked. In contrast, the sheet nacre has a more random staggered arrangement with no well-defined overlap and core regions [34]. Although the interfaces of the edge faces of the upper platelets are cracked, the platelets under the interfaces can effectively resist further cracking. The regular arrangement of columnar

nacre suffers a more significant effect of contact pressure, which makes a larger deformation. Therefore, the likelihood of friction and wear in sheet nacre is lower than that in columnar nacre.

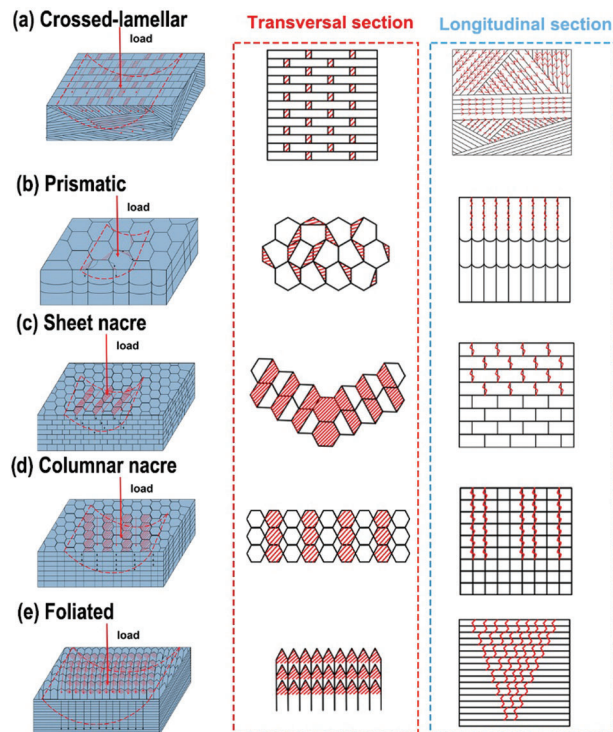


Figure 9: Schematic diagrams showing the abrasion mechanisms in crossed-lamellar (a), prismatic (b), sheet nacre (c), columnar nacre (d), and foliated structure (e). Notes that the red line represents the worn area

The foliated structure is composed of blade-like elongated parallel crystals of calcite (lamellae) that are coalesced laterally to form flakes (folia) with arrow-point [35]. Because the foliated structure is composed of blade-like slats that are extremely thin, the structure is particularly susceptible to fracture wear and even more severe failure (Fig. 9e). Therefore, the foliated structure exhibits the worst tribological behavior.

To summarize, although the hardness of the prismatic is not large, it presents the best resistance to friction and wear deformation among the five common types of structures in mollusk shells. In nature, the microstructures and mechanical properties of materials are mainly dominated by their functions. The prismatic layer, as the outer layer in shells, should resist the wear and friction of the water and sand. For this reason, it must present excellent wear and friction resistance to protect the biological shells. In this work, the wear resistance of the microstructures is determined by the organic matrix, arrangement, and basic building block. More specifically, the squeezing action of force and normal load will produce different stress concentrations due to the varied structural arrangement and basic building block in different microstructures, which leads to the difference in anti-wear and wear morphologies. The above research findings provide an essential guideline for the biomimetic fabrication of friction-reduction and anti-wear materials.

4 Conclusion

The friction behaviors of cross-lamellar, prismatic, sheet nacre, columnar nacre, and foliated structures were investigated systematically in the present work. The following conclusions can be drawn:

1. The cross-lamellar and foliated structures have a severely worn surface with fatigue fracture and plastic deformation, and fracture failure emerges almost on all of the edges in the foliated structure. For nacreous structures, the anti-wear ability of columnar nacre is greater than that of sheet nacre. In sharp contrast, the prismatic structure possesses excellent friction resistance, which explains why the prismatic structure is frequently located on the exterior surface of shells.
2. Unlike metals, there is no perfect positive correlation between anti-wear capacity and hardness in mollusk shells. The wear resistance properties of different microstructures are closely dependent upon the interactions of the organic matrix, structural arrangement, and basic building block.

As a low-cost renewable resource, mollusk shells have large potential value. Based on the above results, the prismatic structure can be reused in conditions with more wear and friction damage. The nacreous structures can be used in handicrafts and building materials as they have beautiful colors and higher hardness. The foliated structure presents a highly transparent feature, but it has a poor wear and friction resistance. Thus, it is beautiful as handicrafts and ornaments.

Funding Statement: This work was supported by the National Natural Science Foundation of China (Grant No. 51902043), and the Fundamental Research Funds for the Central Universities (Grant Nos. N2102007, N2102002, and N2202011). This work was also partially supported by the National Natural Science Foundation of China (Grant Nos. 51871048 and 52171108).

Author Contributions: **Xin Wang:** Conceptualization, Methodology, Data curation, Formal analysis, Investigation, Writing—original draft. **Ying Yan:** Methodology, Roles—review & editing. **Hongmei Ji:** Funding acquisition, Methodology, Roles—review & editing. **Xiaowu Li:** Funding acquisition, Methodology, Resources, Supervision, Roles—review & editing.

Conflicts of Interest: The authors declare that they have no conflicts of interest to report regarding the present study.

References

1. Ram Chandar, K., Hegde, C., Yellishetty, M., Gowtham Kumar, B. (2015). Classification of stability of highwall during highwall mining: A statistical adaptive learning approach. *Geotechnical and Geological Engineering*, 33(3), 511–521. <https://doi.org/10.1007/s10706-014-9836-6>
2. Sameoto, D., Khungura, H., Benvidi, F. H., Asad, A., Liang, T. S. et al. (2022). Chapter Fifteen—Space applications for gecko-inspired adhesives. In: *Biomimicry for aerospace*, pp. 423–458. <https://doi.org/10.1016/B978-0-12-821074-1.00016-5>
3. Goswami, A. (2021). A comparative study on the mechanical and structural design of nacre in gastropod and bivalve molluscs. *Journal of the Mechanical Behavior of Biomedical Materials*, 114(102), 104212. <https://doi.org/10.1016/j.jmbbm.2020.104212>
4. Massah, J., Fard, M. R., Aghel, H. (2021). An optimized bionic electro-osmotic soil-engaging implement for soil adhesion reduction. *Journal of Terramechanics*, 95(5), 1–6. <https://doi.org/10.1016/j.jterra.2021.01.003>
5. Liang, S. M., Ji, H. M., Li, X. W. (2020). Thickness-dependent mechanical properties of nacre in *Cristaria plicata* shell: Critical role of interfaces. *Journal of Materials Science & Technology*, 44(1), 1–8. <https://doi.org/10.1016/j.jmst.2019.10.039>
6. Li, M., Shi, L. P., Wang, X. L. (2021). Physical mechanisms behind the wet adhesion: From amphibian toe-pad to biomimetics. *Colloids and Surfaces B: Biointerfaces*, 199(6787), 111531. <https://doi.org/10.1016/j.colsurfb.2020.111531>
7. Shan, R., Zhao, C., Lv, P. M., Yuan, H. R., Yao, J. G. (2016). Catalytic applications of calcium rich waste materials for biodiesel: Current state and perspectives. *Energy Conversion and Management*, 127(1), 273–283. <https://doi.org/10.1016/j.enconman.2016.09.018>

8. Currey, J. D., Taylor, J. D. (1974). The mechanical behavior of some molluscan hard tissues. *Zoological Journal of the Linnæan Society*, 173(3), 395–406.
9. Tong, J., Wang, H., Ma, Y., Ren, L. (2005). Two-body abrasive wear of the outside shell surfaces of mollusc *Lamprotula fibrosa* Heude, *Rapana venosa* Valenciennes and *Dosinia anus* Philippi. *Tribology Letters*, 19(4), 331–338. <https://doi.org/10.1007/s11249-005-7450-8>
10. Stempflé, P., Brendlé, M. (2006). Tribological behaviour of nacre-influence of the environment on the elementary wear processes. *Tribology International*, 39(12), 1485–1496. <https://doi.org/10.1016/j.triboint.2006.01.011>
11. Lv, Y., Zhang, X. F., Xiu, W. C., Lei, L. Q., Sun, L. N. (2015). Friction and wear behaviour of *Scapharca subcrenata* under sliding contact conditions as a function of sliding speed and loading level. *4th International Conference on Computer Systems and Communication Engineering: (ICMMCCCE)*, pp. 423–428. Atlantis Press. <https://doi.org/10.2991/icmmcce-15.2015.283>
12. Li, L., Ortiz, C. (2013). Biological design for simultaneous optical transparency and mechanical robustness in the shell of *Placuna placenta*. *Advanced Materials*, 25(16), 2344–2350. <https://doi.org/10.1002/adma.201204589>
13. Li, L., Ortiz, C. (2014). Pervasive nanoscale deformation twinning as a catalyst for efficient energy dissipation in a bioceramic armour. *Nature Materials*, 13(5), 501–507. <https://doi.org/10.1038/nmat3920>
14. Huang, J., Liu, Y., Liu, C., Xie, L., Zhang, R. (2021). Heterogeneous distribution of shell matrix proteins in the pearl oyster prismatic layer. *International Journal of Biological Macromolecules*, 189(31), 641–648. <https://doi.org/10.1016/j.ijbiomac.2021.08.075>
15. An, Y. L., Liu, Z. M., Wu, W. J. (2013). Phase transition of aragonite in abalone nacre. *Phase Transition*, 86(4), 391–395. <https://doi.org/10.1080/01411594.2012.678007>
16. Liang, S. M., Ji, H. M., Li, X. W. (2021). A high-strength and high-toughness nacreous structure in a deep-sea Nautilus shell: Critical role of platelet geometry and organic matrix. *Journal of Materials Science & Technology*, 88(20), 189–202. <https://doi.org/10.1016/j.jmst.2021.01.082>
17. Deng, Z. F., Jia, Z., Li, L. (2022). Biomineralized materials as model systems for structural composites: Intracrystalline structural features and their strengthening and toughening mechanisms. *Advanced Science*, 9(14), 2103524. <https://doi.org/10.1002/advs.202103524>
18. Magrini, T., Bouville, F., Studart, A. R. (2021). Transparent materials with stiff and tough hierarchical structures. *Open Ceramics*, 6(2–3), 100109. <https://doi.org/10.1016/j.oceram.2021.100109>
19. Liu, Y. R., Liu, L. L., Li, S. Y., Wang, R. J., Guo, P. et al. (2022). Accelerated deterioration mechanism of 316L stainless steel in NaCl solution under the intermittent tribocorrosion process. *Journal of Materials Science & Technology*, 121(10), 67–79. <https://doi.org/10.1016/j.jmst.2022.01.011>
20. López-Ortega, A., Bayón, R., Arana, J. L., Arredondo, A., Igartua, A. (2018). Influence of temperature on the corrosion and tribocorrosion behaviour of high-strength low-alloy steels used in offshore applications. *Tribology International*, 121(5), 341–352. <https://doi.org/10.1016/j.triboint.2018.01.049>
21. Castaño, J. G., Botero, C. A., Restrepo, A. H., Agudelo, E. A., Correa, E. et al. (2020). Atmospheric corrosion of carbon steel in Colombia. *Corrosion Science*, 52(1), 216–223. <https://doi.org/10.1016/j.corsci.2009.09.006>
22. Dauphin, Y., Brunelle, A., Cotte, M., Cuif, J. P., Farre, B. et al. (2010). A layered structure in the organic envelopes of the prismatic layer of the shell of the pearl oyster *Pinctada margaritifera* (Mollusca, Bivalvia). *Microscopy and microanalysis*, 16(1), 91–98. <https://doi.org/10.1017/S1431927609991115>
23. Liu, X. J., Li, J. L. (2015). Formation of the prismatic layer in the freshwater bivalve *Hyriopsis cumingii*: The feedback of crystal growth on organic matrix. *Acta Zoologica*, 96(1), 30–36. <https://doi.org/10.1111/azo.12048>
24. Guan, H., Chai, L. J., Wu, J. Y., Gong, X. Y., Xiang, K. et al. (2022). Laser-clad Nb (Ta) TiZr medium-entropy alloy coatings on pure Zr sheet: Microstructural characteristics, hardness and wear resistance. *Intermetallics*, 143, 107498. <https://doi.org/10.1016/j.intermet.2022.107498>
25. Zhou, L., Zhang, J. W., Li, S. Q., Tian, Y., Wang, J. P. et al. (2013). Effects of hardness and grain size on wear resistance of polycrystalline cubic boron nitride. *International Journal of Refractory Metals and Hard Materials*, 17, 105766. <https://doi.org/10.1016/j.ijrmhm.2021.105766>

26. Krishnan, P., Lakshmanan, P., Palani, S., Arumugam, A., Kulothungan, S. (2022). Analyzing the hardness and wear properties of SiC and hBN reinforced aluminum hybrid nanocomposites. *Material Today*, 62(2), 2214–7853. <https://doi.org/10.1016/j.matpr.2022.03.593>
27. Liu, J. Y., Xu, Y. N., Yang, H., Liu, Y. N., Yarlagadda, P. K. D. V. et al. (2020). Investigation of failure mechanisms of nacre at macro and nano scales. *Journal of the Mechanical Behavior of Biomedical Materials*, 112, 104018. <https://doi.org/10.1016/j.jmbbm.2020.104018>
28. Ingrole, A., Aguirre, T. G., Fuller, L., Donahue, S. W. (2021). Bioinspired energy absorbing material designs using additive manufacturing. *Journal of the Mechanical Behavior of Biomedical Materials*, 119(5732), 104518. <https://doi.org/10.1016/j.jmbbm.2021.104518>
29. Ji, H. M., Zhang, W. Q., Li, X. W. (2014). Fractal analysis of microstructure-related indentation toughness of Clinocardium californiense shell. *Journal of the American Ceramic Society*, 40, 7627–7631. <https://doi.org/10.1016/j.ceramint.2013.12.035>
30. Liang, Y., Zhao, Q., Li, X., Zhang, Z., Ren, L. (2016). Study of the microstructure and mechanical properties of white clam shell. *Micron*, 87, 10–17. <https://doi.org/10.1016/j.micron.2016.04.007>
31. Wang, X., Li, P., Cao, X. Q., Liu, B., He, S. W. et al. (2022). Effects of ocean acidification and tralopyril on bivalve biomineralization and carbon cycling: A study of the pacific oyster (*Crassostrea gigas*). *Environmental Pollution*, 313, 120161. <https://doi.org/10.1016/j.envpol.2022.120161>
32. Nalepka, K., Berent, K., Checa, A. G., Machniewicz, T., Harris, A. J. et al. (2022). Ribs of *Pinna nobilis* shell induce unexpected microstructural changes that provide unique mechanical properties. *Materials Science and Engineering: A*, 829(1), 142163. <https://doi.org/10.1016/j.msea.2021.142163>
33. Ding, Z. Q., Duan, Y. G., Xiao, H., Wang, B. (2022). Bio-inspired self-stitching discontinuous fiber reinforced composites with enhanced ductility and energy absorption. *Composites Communications*, 34, 101261. <https://doi.org/10.1016/j.coco.2022.101261>
34. Goswami, A. (2021). A comparative study on the mechanical and structural design of nacre in gastropod and bivalve molluscs. *Journal of the Mechanical Behavior of Biomedical Materials*, 114(102), 104212. <https://doi.org/10.1016/j.jmbbm.2020.104212>
35. Checa, A. G., Yáñez-Ávila, M. E., González-Segura, A., Varela-Feria, F., Griesshaber, E. et al. (2019). Bending and branching of calcite laths in the foliated microstructure of pectinoidean bivalves occurs at coherent crystal lattice orientation. *Journal of Structural Biology*, 205(3), 7–17. <https://doi.org/10.1016/j.jsb.2018.12.003>